Towards the use of acrylic acid graft-copolymerized plant biofiber in sustainable fortified composites

Rana, Ashvinder K.; Thakur, Vijay Kumar; Singha, Amar S.

Published in:
E-Polymers

DOI:
10.1515/epoly-2021-0080

First published: 12/11/2021

Document Version
Publisher's PDF, also known as Version of record

Research Article

Ashvinder K. Rana*, Vijay Kumar Thakur*, and Amar S. Singha

Towards the use of acrylic acid graft-copolymerized plant biofiber in sustainable fortified composites: Manufacturing and characterization

https://doi.org/10.1515/epoly-2021-0080
received June 17, 2021; accepted September 07, 2021

Abstract: In this study, the impact of particle form of the *Cannabis indica* plant *biofibers* and the fiber's surface tailoring on the physical, thermal, dielectric, and mechanical properties of unsaturated polyester composite specimens manufactured utilizing nonconventional materials were investigated. The mechanical properties such as compressive, flexural, and tensile strengths of the composite specimens were noticed to increase after functionalization of biofiber with acrylic acid and maximum enhancement was found at 20% of biofiber sacking. The physical characterization was concentrated on the assurance of the dielectric constant, dielectric strength, dielectric loss, moisture absorption, chemical resistance, percentage of swelling, limiting oxygen index, and biodegradation of polymer composites under red soil. An increase in dielectric strength from 28 to 29 kV, limiting oxygen index values from 19% to 23%, and moisture/water absorption behavior was noted for resulted bio-composites after surface tailoring of biofiber. To assess the deterioration of the polymeric materials with the temperature, differential scanning calorimetric and the thermogravimetric tests were carried out and enhancement in thermal stability was noted after fortification of polyester composites with functionalized biofiber.

Keywords: graft copolymers, acrylic acid, biocomposites, dielectric strength, mechanical strength

1 Introduction

Polymers and polymer composites are at present among the most continuously growing materials and there can be no uncertainty that they are vital to present engineering society (1–5). In the last few years, investigation into these polymeric materials has not only been directed on exceptionally tough and durable polymer composites, yet additionally on inexhaustible, biocompatible, biodegradable, and sustainable biomaterials (6–10). The primary drawback of synthetic fiber invigorated composite materials is that two distinctive synthetic components of the framework make their recycling or reuse significantly confounded and high energy is needed for their development. Different kinds of biomass such as plant fibers are a type of biocompatible and sustainable materials that could be utilized to develop biodegradable materials including composites that satisfy cost, density, and strength requirements (11–14). An enormous number of biofibers such as banana, sisal, coir, *Grewia optiva*, hemp fibers, and so forth have been investigated and utilized for the development of composite materials (15–18). Each fiber has explicit attributes that influence its reinforcement ability and contribution to the fabrication of composite materials (19–21). In addition, utilization of plant fibers for fortification of thermosetting/thermoplastic matrix gives multiple advantages, such as easy availability, budget-friendly, low density, biodegradability, ease of processing, high tensile strength, and good thermal properties (20,22,23). *Cannabis indica* fiber (CIF), which is also known as Indian hemp fibers, is one of the toughest and stiffest plant fibers

*** Corresponding author: Ashvinder K. Rana,** Department of Chemistry, Sri Sai University, Palampur, 176061, India; Department of Chemistry, Maharishi Markandeshwar University, Mullana, Haryana, 133-207, India, e-mail: ranaashvinder@gmail.com, ranaashvinder2020@gmail.com
*** Corresponding author: Vijay Kumar Thakur,** Biorefining and Advanced Materials Research Center, SRUC, Edinburgh, United Kingdom; Department of Mechanical Engineering, School of Engineering, Shiv Nadar University, Uttar Pradesh, 201314, India; School of Engineering, University of Petroleum & Energy Studies (UPES), Dehradun, Uttarakhand, India, e-mail: Vijay.Thakur@sruc.ac.uk
Amar S. Singha: Department of Chemistry, National Institute of Technology, Hamirpur, 177005, India

and has a considerable perspective as a composite fortifying agent (24–26). The Indian hemp bast fibers are made up of approximately 70–74% cellulose, 15–20% hemicelluloses, 4% lignin, 1% pectin, and 1–2% waxes (27). The process of extraction of fibers from stalks is known as retting. There are different kinds of retting methods namely chemical retting, enzymatic retting, water retting, dew retting, and mechanical retting (28,29). Even though the usage of plant fibers as a strengthener in composite materials gives different advantages, the innate properties of plant fibers prompt some undesired qualities to the composites. Väisänen et al. (30) recognized four significant difficulties that can extensively limit the utilization of plant materials in composites: restricted mechanical strength, abundant water absorption, low imperviousness to fire, and lack of homogenous distribution of biofibers due to hydrophilic nature. The parameters which control properties of plant fiber are the collection time, type of retting, fiber processing technique employed, and the type of soil wherein the fiber plant is developed (31–33). Efforts have been made by several researchers for controlling the impact of aforementioned challenges of biofiber-fortified polymer composites by employing different types of enzymatic, physical, and chemical techniques (34–36). Banea et al. (35) reviewed the impact of different chemical treatments such as alkali treatment, silane, graft copolymerization, etc., on the properties of resulted biopolymer composites. They reported a considerable improvement in mechanical, thermal, and physico-chemical properties after surface functionalization of biofiber. A large number of physical methods such as plasma treatment, dielectric barrier technique, corona treatment, and ultrasound/ultrasonic treatment have also been successfully employed to enhance the properties of biofiber-fortified polymer composites (36). Further, various types of thermosetting and thermoplastic matrices are available in the market and have been utilized for the fabrication of polymer composites (37). Among the different thermosetting matrices, unsaturated polyester (UPE) resins are the most conspicuous, cheap, and universally utilized in numerous applications where benefits might be taken from their wide range of mechanical qualities, better erosion resistance, and low density (38). Polyester matrices were likewise utilized for coatings, body fillers, developing marble, polyester concrete, cladding boards, roofing tiles, pipes, and bathroom furniture such as shower plates. Conzatti et al. utilized particle forms of wool fiber for reinforcing polyester composites (39). They further evaluated the thermal, morphological, and dynamic mechanical analysis of resulted composites. Prasad and Rao studied the impact of three different biofibers i.e., sisal, jowar, and bamboo on the resulted properties of polyester composites (40). Chabros et al. stated an increase in mechanical properties of microcrystalline cellulose-fortified UPE composites after the esterification of cellulosic fiber using methacrylic anhydride (41). Singha et al. studied the impact of different biofibers' surface modification approaches such as alkali treatment, benzoylation, silane, and acrylonitrile grafting onto dielectric, thermal, and mechanical qualities of *Grewia optiva* plant fiber-fortified UPE composites (42). In addition, Singha and Rana also utilized silane and acrylonitrile grafted CIFs for the reinforcement of polyester composites (26). An increase in overall properties of polymer composites has been reported by them. Since no work has been reported on surface functionalization onto CIFs using acrylic acid (AAc) and their subsequent utilization in particle form for fabrication of polymer composites, the present study aims to assess the impacts of AAc graft copolymerization on mechanical, thermal, and dielectric properties of particles of Indian hemp fiber-reinforced polyester composites.

2 Experimental methods

2.1 Materials

CIFs, after its collection from local sources of Himachal Pradesh, was at first cleansed with 2% of washing powder solution and afterwards dried in an oven. The dried CIFs were then soxhlet extracted with C_2H_6CO for 60–72 h and subsequently washed with water and air-dried to get rid of wax and other water dissolvable contaminants. Ceric ammonium nitrate (CAN), AAc and magnesium hydroxide, and zinc borate of Merck made were used as initiator, monomer, and fire retardants, respectively. Further, purification of monomer was done by distillation under reduced pressure. UPE was supplied by Crystic Resins India Pvt. Ltd. and Cobalt naphthenate (CN) and methyl-ethyl-ketone-peroxide (MEKP) were used as accelerators and hardeners, respectively. The weighing of chemicals and samples was carried out on Libror AEG-220 (Shimadzu) electronic balance. Moisture absorption was studied in the humidity chamber of Swastika makes.

2.2 Methods

2.2.1 Synthesis of CIFs-*g*-poly(AAc) graft copolymers

Graft copolymers were synthesized as per the procedure reported by Singha and Rana (43) (Figure 1). The CIFs were initially chopped into a particle size of 90 μm and

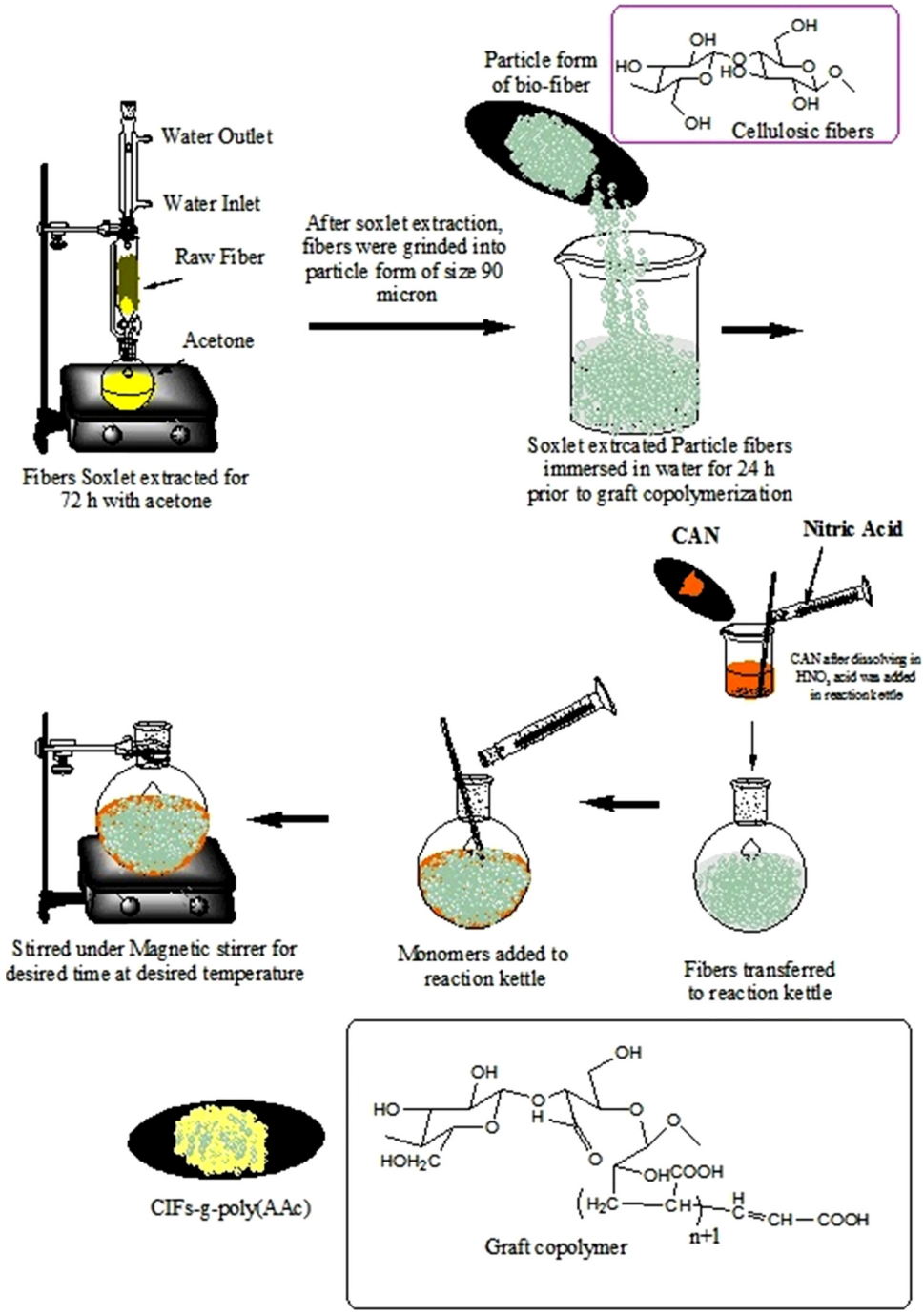

Figure 1: Shows the scheme for the preparation of CIFs-*g*-poly(AAc) graft copolymers.

then subsequently dipped into water for 20–24 h. Afterwards, the fibers were transferred to the reaction kettle and a known quantity of CAN (1.82×10^{-2} mol·L^{-1})/HNO_3 (3.60×10^{-2} mol·L^{-1}) initiator system and AAc monomer (2.91×10^{-1} mol·L^{-1}) were added to the kettle and the mixture was stirred continuously for 120 min at 45°C. The graft-copolymerized biofibers were then filtered, cleaned with hot water, and finally dried.

2.2.2 Composites fabrication

Different weight proportions (10%, 20%, 30%, and 40%) of raw and surface functionalized CIFs were utilized for the development of UPE matrix-based biocomposites by using the conventional hand lay-up succeeded by a compression molding technique. A stainless steel mold of dimension 150 mm × 150 mm × 5 mm has been used for

the preparation of composite specimens. 2% each of CN and MEKP were used as accelerator and hardener, respectively, for developing polymer composites and were mixed thoroughly in the polyester resin before fortification. Further, upon inclusion of particle form of raw and graft-copolymerized CIFs, the blend was stirred to achieve equal proliferation of the fibers in the resin, which requires utmost care as hydrophilic cellulosic fibers tend to agglomerate. The composite sheets were cured for 12 h under the pressure of 100 kg·cm^{-2}, which were subjected to post-curing in the air for 24 h. Composite specimens of suitable dimensions as per the ASTM standards were utilized for mechanical, dielectric, and physico-chemical testing.

2.2.3 Estimation of physico-chemical properties of polymer composites.

Water absorption, stability against chemicals, and moisture absorption behavior of biocomposite specimens were studied as per the methods reported by Singha et al. (42).

2.2.3.1 Water absorption

Percent water absorption was evaluated by dipping preweighted pure UPE and UPE matrix-based composite samples of size 10 mm × 10 mm × 2 mm in distilled water for 60 days. The samples were removed from the water after a gap of 10 days each and were dried subsequently with the help of filter papers to eliminate the surplus water and then weighed again. The percent water absorption was determined utilizing Eq. 1:

$$W_a = \left(\frac{W_{fin} - W_{int}}{W_{int}}\right) \times 100 \quad (1)$$

where W_a, W_{fin}, and W_{int} are percent water absorption, final weight, and initial weight, respectively.

2.2.3.2 Chemical stability

The stability against chemicals of polymer composites was studied by immersing dried specimens in HCl and NaOH solutions of different normality for a specified time ranging between 10 and 30 days. Afterwards, the solution was decanted off; specimens were cleaned with purified water, seared in an oven, and weighed. The % chemical stability (P_{cs}) was evaluated in respect of weight reduction by utilizing Eq. 2:

$$\text{Perecent chemical stability } (P_{cs}) = \frac{W_{int} - W_{ac}}{W_{int}} \times 100 \quad (2)$$

where W_{int} is the initial weight and W_{ac} is the weight after the specified interval.

2.2.3.3 Moisture absorption

The dampness behavior of pure matrix and its polymer composites were studied in a humidity chamber (Swastika India made) by placing known weights (W_{int}) of dried samples at 20%, 50%, and 80% of relative humidity for 8 h. The final weights (W_{fin}) of specimens were noted instantaneously after removing from the chamber after the specified time. The % dampness was evaluated as per Eq. 3:

$$\%\ \text{Dampness} = \frac{W_{fin} - W_{int}}{W_{int}} \times 100 \quad (3)$$

2.2.4 Biodegradation study

The soil burial method was utilized to evaluate the biodegradation of the polyester composites. The samples of dimension 10 mm × 10 mm × 10 mm were covered under red soil in a pot for a time of 6–12 months and were presented to various atmospheric conditions all over the year. Before the soil interment test, samples were dried and the preliminary weight (W_{int}) was noted. After concealing the samples for a predefined time, the specimens were removed, cleaned with water, and dried again in an oven to obtain a constant weight. The weights (W_{fin}) of samples were recorded again and percent weight reduction (W_{pwl}; %) biodegradability was ascertained by Eq. 4:

$$W_{pwl} = \left(\frac{W_{int} - W_{fin}}{W_{fin}}\right) \times 100 \quad (4)$$

2.3 Evaluation of mechanical properties

The compressive, flexural, and tensile strengths of raw and CIFs-*g*-poly(AAc) strengthen UPE composites of dimensions 10 cm × 10 cm × 0.5 cm were studied on a universal testing machine (Hounsfield H25KS) as per the ASTM D3410, ASTM D790, and ASTM D3039, respectively. For testing purposes, three samples of each of the polymer composite sheets were utilized and average data have been reported. Further, mechanical properties of all composite samples were

investigated at a strain rate of 10 mm·min^{-1} and stress was continued till complete failure of samples.

2.4 Characterization

2.4.1 Fourier transform infrared spectroscopy (FTIR)

FTIR spectra of pure matrix and its polymer composites were acquired on Perkin Elmer infrared spectrophotometer in the range of 400–4,000 cm^{-1}.

2.4.2 Scanning electron microscopy

Scanning electron microscopy (SEM) investigation of composite specimens was done on an LEO 435 VP scanning electron microscope, after sputtering composite specimens with gold. All the SEM images were captured at a magnification of 1,000×.

2.4.3 Thermal gravimetric analysis (TGA) and differential scanning calorimetric (DSC) analysis

TGA and DSC analysis of pure matrix and raw CIFs and CIFs-*g*-poly(AAc) co-polymers-fortified polyester composite samples were done using Mettler Toledo TGA/DSC instrument in a nitrogen atmosphere with a flow rate of 20 mL·min^{-1} at a heating rate of 15°C·min^{-1} and 10°C·min^{-1}, respectively. Further, the temperature was scanned from 20°C to 800°C in the case of TGA and from 20°C to 500°C in the case of DSC studies.

2.4.4 Dielectric properties

The different properties of composite samples were analyzed utilizing Wayne Kerr 6500B LCR impedance analyzer at 30°C in the frequency range from 0 to 1×10^6 Hz. The composite specimens of dimensions 10 mm × 10 mm × 2 mm were utilized for ascertaining the dielectric properties. The test specimen after coating with silver paste and drying in the air were used as formal electrodes by fixing copper wires on both sides of the samples.

2.4.5 Dielectric strength

The breakdown voltage and dielectric stability of composite specimens were evaluated in a Hipot 60 kV instrument set specially designed for analyzing insulation characteristics of solid materials. The testing instrument includes a rectangular-shaped experiment chamber, a control panel, and a transformer. The role of the test chamber, control panel, and high voltage transformer was to carry out electrical breakdown studies of insulating samples, to provide a varying voltage between 0 and 60 kV, and to provide a shield against unexpected short circuits and stumbling off the high voltage when samples under observation fizzle, respectively. Two cylindrical-framed brass electrodes, having a diameter of 51 mm and thickness of 25 mm each have been utilized in the test chamber as per the ASTM standard for examining the insulating sheets. The sample material was placed between brass electrodes and was completely drenched with oil of superior quality for smooth investigation of electrical breakdown and to control circuit failure.

2.4.6 Limiting oxygen index (LOI)

The LOI of pure resin and different composite specimens was evaluated according to ASTM D-2863-77 in an LOI-smoke-230 Oxygen Index instrument of Dynsco Company. Further, impacts of zinc borate $Zn_3(BO_2)_3{\cdot}5H_2O$ and Magnesium hydroxide $Mg(OH)_2$ fire retardant fillers on LOI values of composite specimens were also studied. Samples of size 100 mm (length) × 6 mm (width) × 3 mm (thickness) were utilized for LOI testing. For measurement of LOI values, the test specimen was mounted on a specimen holder and ignited well with flame till it catches fire properly and then the lowest percentage of oxygen level was measured that will lead to the 50 mm of samples being burned continuously or will cause the specimens to burn for 180 s, whichever will be earlier. During testing, the level of oxygen was varied approximately by 0.2% depending on whether the samples continued to burn or not. Three samples of each material have been characterized at different oxygen/nitrogen flow rates.

3 Results and discussion

3.1 Mechanical properties

The assorted mechanical properties such as compressive, flexural, and tensile strengths of raw and CIFs-*g*-poly (AAc) strengthen UPE composites have been displayed in Table 1.

Table 1: Mechanical properties of CIFs fortified polymer composites

Sample name	Tensile strength (MPa)	Compressive strength (MPa)	Flexural strength (MPa)	Percent elongation (%)
Virgin UPE	18.70 ± 0.62	31.25 ± 0.71	51.70 ± 0.86	4.02 ± 0.22
UPE-Rnf-10 wt% of raw CIFs	22.66 ± 0.75	35.60 ± 1.32	54.90 ± 2.45	3.61 ± 0.12
UPE-Rnf-20 wt% of raw CIFs	23.39 ± 0.62	38.18 ± 1.66	56.21 ± 2.89	2.61 ± 0.16
UPE-Rnf-30 wt% of raw CIFs	21.80 ± 0.88	36.48 ± 1.49	55.70 ± 3.02	2.40 ± 19
UPE-Rnf-40 wt% of raw CIFs	19.30 ± 0.78	35.72 ± 1.98	54.40 ± 2.45	2.14 ± 0.21
UPE-Rnf-10 wt% of CIFs-*g*-poly(AAc)	23.58 ± 0.95	41.40 ± 1.55	58.96 ± 3.22	3.78 ± 0.33
UPE-Rnf-20 wt% of CIFs-*g*-poly(AAc)	24.49 ± 0.58	42.10 ± 1.47	62.10 ± 2.06	2.48 ± 0.29
UPE-Rnf-30 wt% of CIFs-*g*-poly(AAc)	23.02 ± 0.77	37.08 ± 1.98	56.59 ± 2.41	2.40 ± 0.26
UPE-Rnf-40 wt% of CIFs-*g*-poly(AAc)	21.60 ± 0.86	35.5 ± 2.06	53.70 ± 2.19	1.82 ± 0.31

Pure UPE samples have been noticed to have a maximum tensile strength of 18.7 MPa, compressive strength of 31.25 MPa, flexural strength of 51.7 MPa, and percent elongation of 4.02%. The mechanical strength of the UPE matrix has been noticed to enhance fortification with raw CIFs, which were found to be further improved after functionalization of CIFs with AAc. After analyzing the results, it can be concluded that mechanical properties of both virgin and functionalized CIFs-fortified UPE composites improve with the increase in fiber stacking and were observed to be maximum at 20% of fiber stacking. However, a decline in mechanical behavior has been noticed after an increase in percent stacking beyond 20%. Further, a noticeable improvement in compressive, tensile, and flexural toughnesses of UPE composites has been observed upon fortification with CIFs-*g*-poly(AAc) fibers than raw fibers. This observance in the behavior of CIFs-*g*-poly(AAc)-fortified UPE matrix-based composites could be due to the enhancement in surface roughness onto CIFs after surface functionalization which may result in better wetness ability and adhesion with the matrix.

It has also been noticed that raw CIFs-fortified UPE polymer composites exhibited a higher percentage of elongation in comparison to CIFs-*g*-poly(AAc)-fortified UPE composites. This behavior may further be associated with improvement in interfacial adhesion between modified fibers and UPE matrix-based materials. In general, it is considered that AAc is a hydrophilic monomer and it may harm the overall mechanical performance of composites; however, no such results have been obtained. This behavior could be assigned due to the formation of hydrogen bonds as well as strong Van der Waals interactions between carbonyl groups of polyester matrix and hydroxyl groups of grafted poly(AAc) chains (Scheme 1).

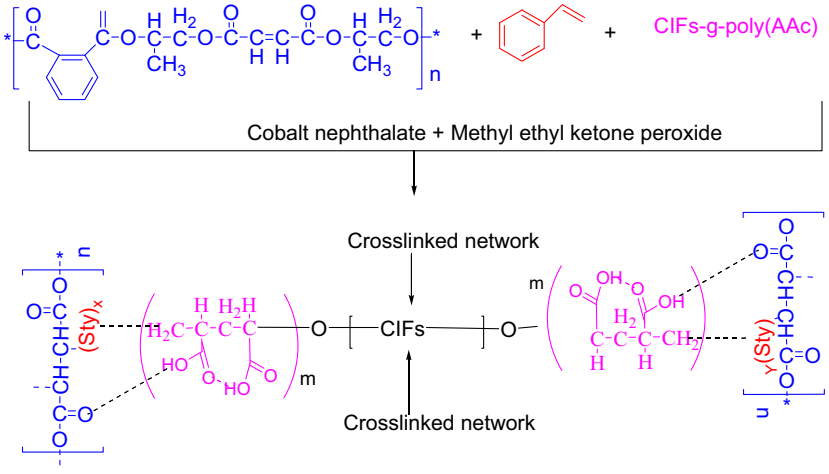

Scheme 1: Scheme shows possible cross-linking between UPE, styrene, and CIFs-*g*-poly(AAc).

3.2 Fourier transforms infrared analysis

The virgin UPE matrix exhibited various peaks at 3431.47, 2,985–2,880, 1738.11, 1600.61 and 1453.48, 1284.69, 1070.97, and at 744.43 and 700.37 cm^{-1}, which have been assigned due to unsaturated C–H stretching, saturated aliphatic hydrocarbon C–H stretching, ester carbonyl group stretching, aromatic ring, in-plane –OH vibrations, due to unsaturated in-plane deformation, and due to out-of-plane bending deformations of aromatic C–H, respectively (Figure 2a–c). However, on fortification of UPE with raw particle CIFs, in addition to the aforementioned peaks, an extra peak at 3,443 cm^{-1} because of O–H stretching of hydrogen-bonded groups has been noticed, which confirms the inclusion of raw CIFs into the UPE matrix. Further, on reinforcement with graft copolymers, an enhancement in the intensity of peaks at 1,600, 1728.95, and 1,285 cm^{-1} has been observed because of the unsaturated (–CH–=CH–) groups stretching, C=O stretching of pendant COOH groups present in grafted poly AAc chains, and due to –C–H rocking (–CH=C(COOH)–), respectively.

3.3 SEM

It is a phenomenal method for inspecting the surface characteristics of composite samples. After evaluating

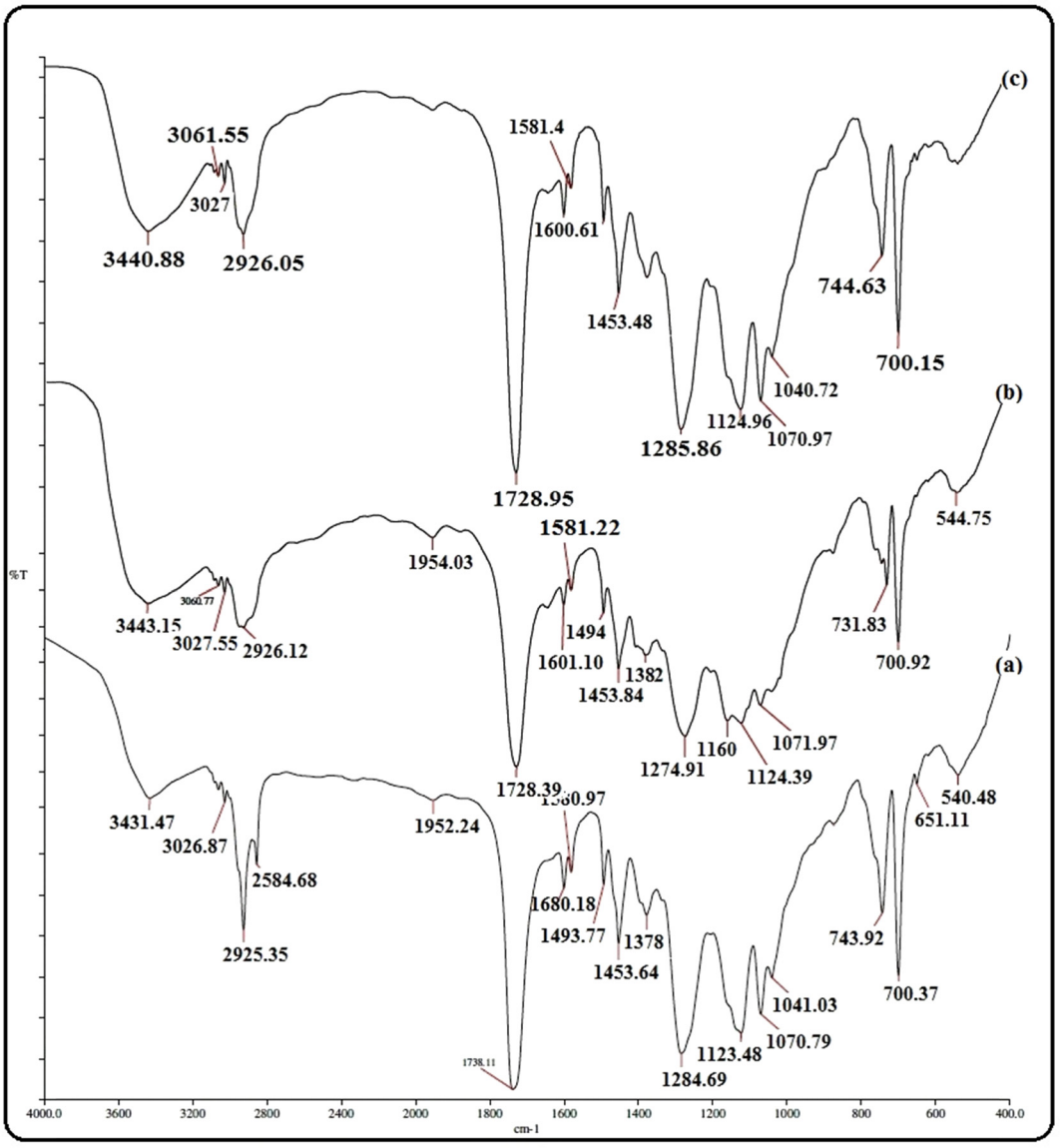

Figure 2: FTIR spectra of (a) pure UPE, (b) CIFs-Rnf-polyester, and (c) CIFs-*g*-poly(AAc)-Rnf-polyester composite specimens.

the SEM micrographs (Figure 3) of pure UPE resin and polymer composites fortified with raw and AAc graft-copolymerized CIFs, it has been seen that the morphology of pure UPE resin is unique in relation to its polymer composites fortified with raw and CIFs-*g*-poly(AAc) copolymers in respect of smoothness and coarseness. In addition, a poor interfacial adhesion was noted in-between raw CIFs and matrix and has been noticed to be enhanced upon graft copolymerization of CIFs with AAc monomer because of the better-wettability of fibers and matrix.

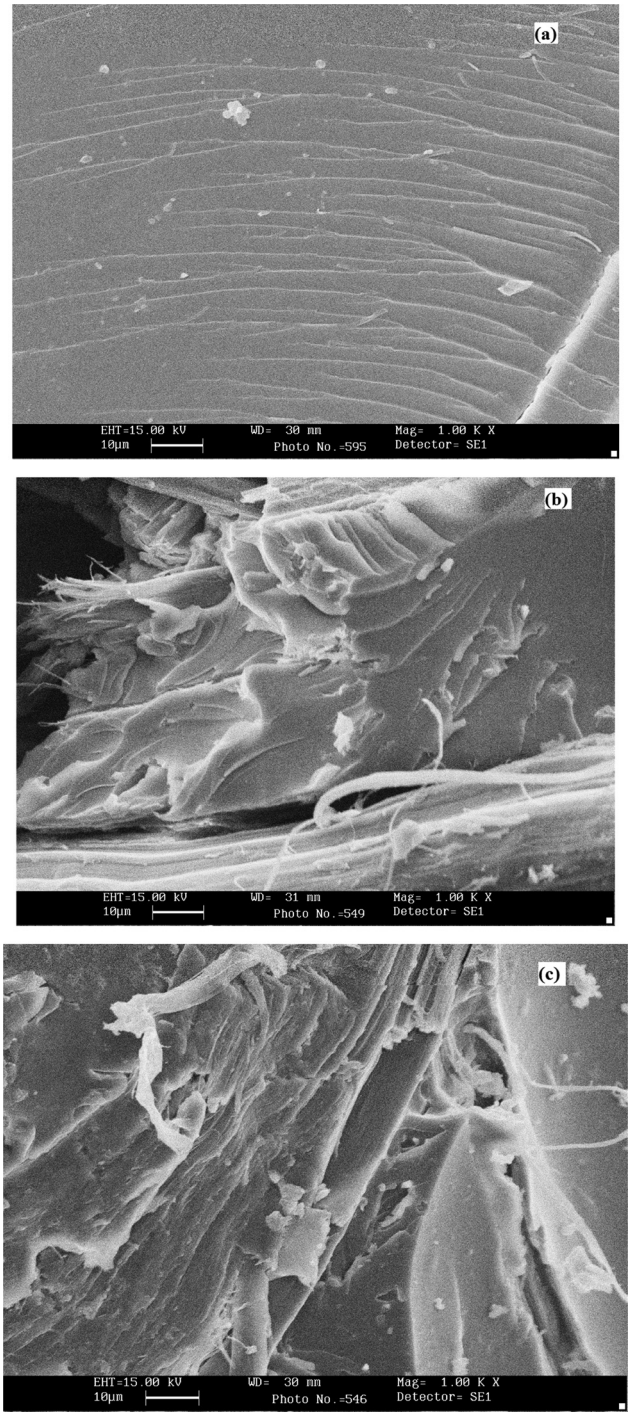

Figure 3: SEM images of (a) virgin matrix, (b) CIFs-Rnf-polyester, and (c) CIFs-*g*-poly(AAc)-Rnf-polyester matrix-based polymer composites.

3.4 Thermal analysis

The thermal behavior of pure matrix and UPE composite samples fortified with raw CIFs and CIFs-*g*-poly(AAc) copolymers have been depicted in Figure 4.

3.4.1 TGA

This technique measures the thermal stability of materials in terms of weight loss with respect to applied temperature. In the case of the virgin polyester matrix, single-stage deterioration was observed in-between

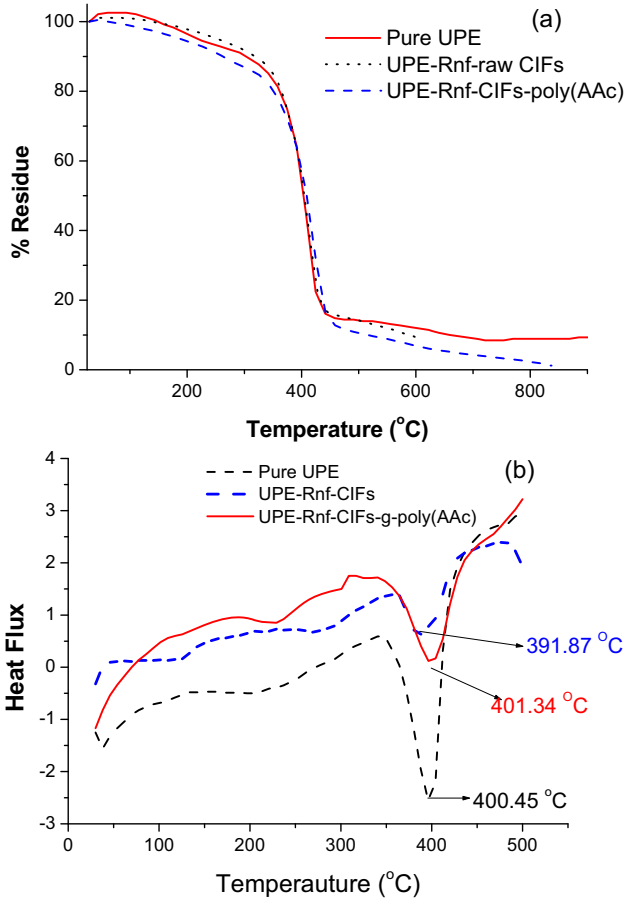

Figure 4: (a) TGA and (b) DSC curves of different composite samples.

270°C and 450°C. The initial decomposition temperature (IDT) and final decomposition temperature (FDT) of the pure matrix, CIFs-Rnf-UPE, and CIFs-*g*-poly(AAc)-Rnf-UPE composite specimens have been noted to be 325.05°C and 441.48°C, 330.68°C and 438.09°C, and 329.29°C and 458.54°C, respectively, (Figure 4a). From this data, we can conclude that CIFs-*g*-poly(AAc) degrade to a lesser extent than raw fiber composites. Also, on looking at the degradation temperature (DGT) of the virgin matrix, raw CIFs-fortified polyester composites, and CIFs-*g*-poly(AAc)-fortified polyester composites at 90%, 55%, and 20% of weight loss, it can be concluded that surface-modified CIFs strengthen polyester composites are highly stable than raw CIFs' strengthen composites and neat matrix. The better thermal quality of CIFs-*g*-poly(AAc) strengthen composites could be because of extra Van der Waals and hydrogen bonding between fiber and matrix. Further, the increase in the thermal behavior of UPE matrix-based polymer composites after graft copolymerization of AAc onto CIFs has been supported through DSC studies.

3.4.2 DSC analysis

In this technique, the difference in the amount of heat needed to raise the temperature of the reference and sample is measured with respect to applied temperature and is a more advanced technique for analyzing the thermal quality of polymeric materials. An endothermic peak was observed for all composite specimens because of the disruption of the glassy empire of the polymer network (Figure 4b). The different thermal parameters such as the temperature of decomposition (T_d), enthalpy of reaction (ΔH_R), and levels/degree of crystallinity (X_c) of CIFs and CIFs-*g*-poly(AAc)-fortified polyester composites were evaluated from DSC curves, and outcomes have been summed up in Table 2. The extent of crystallinity was estimated by using Eq. 5:

$$\text{Degree of crystallinity } (X_c) = \frac{\Delta H_R \times 100}{\Delta H_R^{\circ} \times W} \qquad (5)$$

where W is the mass proportion of matrix in the composite specimens and ΔH_R° is the enthalpy of reaction for hundred percent crystalline UPE matrix which has been taken to be 400 J·g^{-1} (44).

The thermal parameters have been noted to be affected by the type of fillers used i.e., raw or surface-modified fillers. From the table, we can conclude that T_d of CIFs-fortified polyester composites enhances after functionalization of CIFs. The significant increase in thermal quality of surface-tailored CIFs-fortified polymer composite could be

Table 2: TGA/DSC data of neat UPE, UPE-Rnf-raw CIFs, and UPE-Rnf-CIFs-*g*-poly(AAc)

Sample designation	TGA data						DSC data		
	IDT (°C); wt% loss	FDT (°C); wt% loss	DGT (°C) at 20 wt% loss	DGT (°C) at 55 wt% loss	DGT (°C) at 90 wt% loss	Residual weight (%) at 900°C	T_d (°C)	ΔH_R	Degree of crystallinity (X_c)
Neat UPE	325.05; 12.28	441.48; 83.89	358.21	407.82	671.79	9.32	400.45	88.14	22.03
UPE-Rnf 20% of raw CIFs	330.68; 11.32	438.09; 82.26	365.03	408.43	592.88	0.59	391.87	110.17	39.34
UPE-Rnf 20% of CIFs-*g*-poly(AAc)	329.29; 10.56	458.84; 81.65	352.14	414.74	525.25	1.24	401.34	121.20	43.28

because of extra intermolecular bonding between CIFs and matrix as the result of surface functionalization. In addition to T_d, surface functionalization has also been found to impact both degrees of crystallinity and ΔH_R of composite specimens. An increment in the crystallinity of virgin UPE matrix after its fortification with raw and surface functionalized CIFs has been noticed. This behavior could be because of the nucleating capability of raw and treated CIFs' fortifying agents for crystallization of UPE. Further, a curtailment in the degree of crystallinity of polymer composites on fortification with CIFs-*g*-poly(AAc) copolymers has also been observed due to the predominance of the non-crystalline region over crystalline after surface functionalization.

4 Dielectric properties

4.1 Dielectric constant, loss, and dissipation factor

Dielectric constant (ε') is a very essential parameter as it provides valuable information regarding the dielectric strength of the insulation material. This parameter is quite helpful in choosing dielectric capacitor material of suitable capacitance for their utility in capacitor banks for electrical power factor enhancement of an electric network installation as it checks the energy dissipated in transmission lines. The ε' of specimens can be calculated by utilizing Eq. 6:

$$\varepsilon' = Ct/\varepsilon_o A, \tag{6}$$

where C is the capacitance, t is the thickness, ε_o is the vacuum permittivity, and A is an area of the specimen under testing. Further dissipation factor ($\tan\delta$), which represents the amount of power dissolute, has been estimated by using Eq. 7:

$$\tan\delta = \varepsilon''/\varepsilon' \quad \text{(here } \varepsilon'' \text{ is the loss factor)} \tag{7}$$

From Figure 5a it has been found that the dielectric constant of raw CIFs-fortified polyester composite specimens is slightly greater than pure UPE, which may be because of the moisture-loving nature of biofibers that will result in enhancement during conductivity of the polyester composite materials. Fundamentally, the water molecules which are absorbed by biofibers from the environment are profoundly polar by nature and thus,

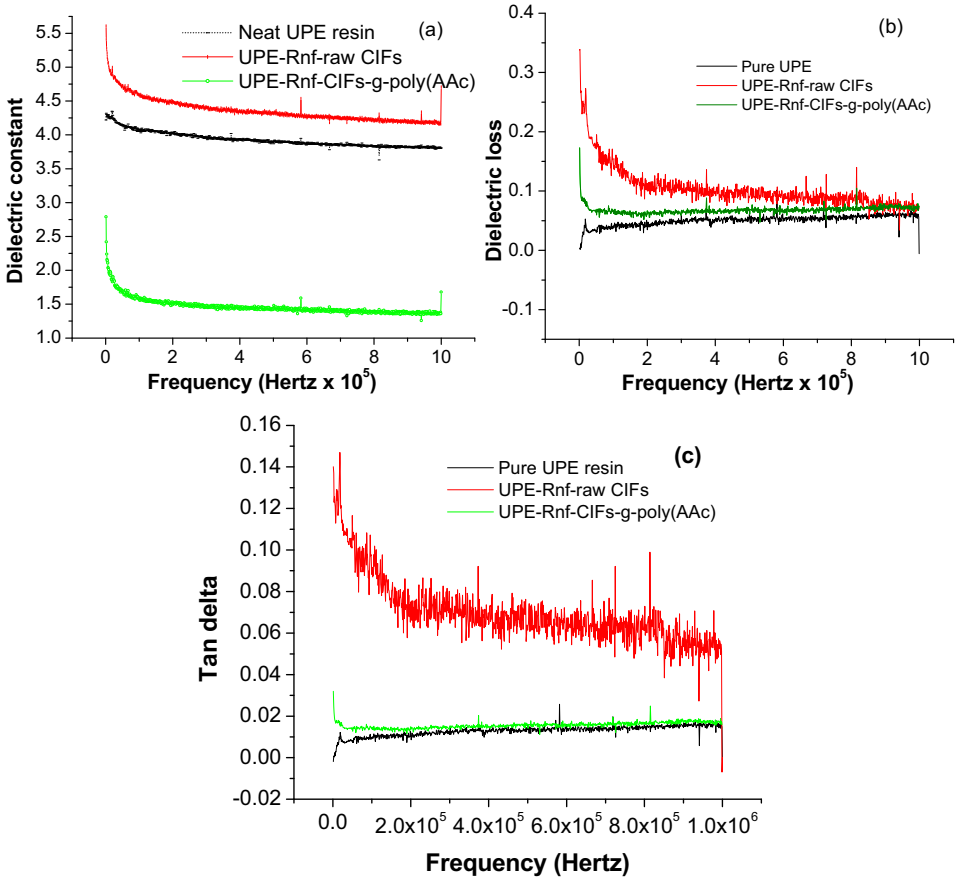

Figure 5: (a) Dielectric constant vs frequency, (b) dielectric loss vs frequency, and (c) tan delta vs frequency for pure polyester matrix and its composites fortified with CIFs and CIFs-*g*-poly(AAc).

Table 3: Dielectric strength and V_b of pure UPE matrix and its polymer composites

Sample Designation	Thickness [t] (mm)	Break down voltage [V_b] (kV)	Withstand voltage (kV)	Dielectric strength (kV·mm^{-1})
Neat UPE	2	34	33	17.00
	4	43	42	10.75
UPE-Rnf 20% of raw CIFs	2	29	28	14.50
	4	35	34	08.75
UPE-Rnf 20% of CIFs-*g*-poly(AAc)	2	30	29	15.00
	4	36	35	09.00

enhance the surface polarization characteristics of specimens and are by and large answerable for such conducts of raw CIFs strengthen UPE bio-composites. However, after fortification of the polyester matrix with CIFs-*g*-poly(AAc) copolymer, a decrement in dielectric constant values due to a decrease in orientation polarization has been observed (45,46).

From Figure 5b and c, it has also been noticed that surface tailoring of fibers additionally reduce the dissipation factor and dielectric loss of biofiber-fortified polymer composites. It may be because of lesser defects and better size after the introduction of poly(AAc) chains onto the surface of the fiber. Nonetheless, there is no specific reason for the aforementioned conduct as dissipation factor or dielectric loss also relies on fiber direction/orientation (47). Since CIFs were irregularly embedded in bio-composite specimens, there might be huge discrepancies in dielectric behavior from one area to another of the samples under study.

4.2 Dielectric strength

The dielectric durability of insulating materials is the least voltage at which it breaks down under the stress of the applied electric field in normal operating conditions. This parameter gives us information about the structural uniformity of the manufactured materials. No doubt, such estimations are not acceptable for designing materials, yet they provide some valuable information regarding the electric stress sustain capability of insulators that will be vital to hold up a specific voltage strength in electrical appliances i.e., in electric motor, power transformer, etc.

The dielectric strength of the composite specimens was figured out by using the following formula:

$$\text{Dielectric strength} = \frac{\text{Breakdown voltage } (V_b)}{\text{thickness (mm)}} \quad (8)$$

Data on the dielectric strength of composite specimens are given in Table 3.

From the table, it can be concluded that the dielectric strength of the raw CIFs and CIFs-*g*-poly(AAc)-fortified composite specimens is on the lower side than the pure UPE matrix. The decrement in strength after fortification with raw CIFs and CIFs-*g*-poly(AAc) might be because of the existence of polar groups on the fibers' surface which promotes the progression of current. Further, between raw CIFs and CIFs-*g*-poly(AAc) strengthen polyester composites, the latter one was noticed to have a little bit better dielectric strength because of the improved

Table 4: Effect of fibers surface functionalization and fire retardants on LOI of UPE/CIFs/Fire retardants composites

UPE:CIFs ratio (% by weight)	Fire retardant (% by weight of UPE)	LOI
Neat UPE	—	20
70% of UPE-Rnf-20% of raw CIFs	—	19
70% of UPE-Rnf-20% of CIFs-*g*-poly(AAc)	—	21
Neat UPE	30% of $Mg(OH)_2$	23
70% of UPE-Rnf-20% of raw CIFs	30% of $Mg(OH)_2$	23
70% of UPE-Rnf-20% of CIFs-*g*-poly(AAc)	30% of $Mg(OH)_2$	23
Neat UPE	30% of zinc borate	22
70% of UPE-Rnf-20% of raw CIFs	30% of zinc borate	22
70% of UPE-Rnf-20% of CIFs-*g*-poly(AAc)	30% of zinc borate	23

interactions between the matrix and surface-modified fibers. The pattern acquired in the case of the study of dielectric strength was found to be consistent with the trends got during the investigation of dielectric constant and the dielectric loss of polymeric materials.

5 LOI test

The data on impacts of CIFs, CIFs-*g*-poly(AAc) loading, and inclusion of different fire retardants on LOI values of resulted polyester bio-composites are given in Table 4. A decrement in LOI values of the neat UPE matrix has been found after fortification of the UPE matrix with raw CIFs because of the highly flammable nature of CIFs. However, after fortification of the UPE matrix with CIFs-*g*-poly (AAc), LOI values increase because of the increment in combustion temperature. The results obtained were discovered to be following line with DSC/TGA results, which likewise support better thermal quality of CIFs-*g*-poly (AAc) copolymer-fortified UPE composites.

Further, an enhancement in LOI values of UPE matrix-based composites was investigated when fire retardants (magnesium hydroxide/zinc borate) were utilized as fillers. Maximum fire retardency was found in the case of magnesium hydroxide-filled polymer composites because of their better thermal quality than zinc borate (48). On the utility of magnesium hydroxide/zinc borate in combination with raw CIFs and CIFs-*g*-poly(AAc) as a fortifying agent, the LOI values i.e., fire retardant characteristics of resulted composite specimens have been noticed to be further enhanced.

6 Physico-chemical properties

Data on water absorption, chemical resistance behavior, and moisture absorption behavior are given in Tables 5–7, respectively.

Table 5: % Water absorbance by neat UPE, UPE-Rnf-raw CIFs, and UPE-Rnf-CIFs-*g*-poly(AAc)

Sample designation	After number of days				
	10	20	30	40	50
Virgin UPE	0.01	0.09	0.19	0.99	1.65
UPE-Rnf-20% of raw CIFs	3.95	5.74	6.98	7.76	7.94
UPE-Rnf-20% of CIFs-*g*-poly(AAc)	3.92	5.71	6.12	6.80	7.02

Table 6: % Chemical resistance shown by neat UPE, UPE-Rnf-raw CIFs, and UPE-Rnf-CIFs-*g*-poly(AAc) against base and acid solution after different number of days

Sample designation	Against NaOH						Against HCl					
	wt% reduction against 1.0 N			wt% reduction against 3.0 N			wt% reduction against 1.0 N			wt% reduction against 3.0 N		
	10 days	20 days	30 days	10 days	20 days	30 days	10 days	20 days	30 days	10 days	20 days	30 days
Virgin UPE	0.39	2.42	4.76	6.95	9.06	12.2	0.000	0.041	0.070	0.121	0.189	0.274
UPE-Rnf-20% of raw CIFs	0.81	7.05	11.42	16.93	29.72	35.55	0.0088	0.0814	0.2766	0.2898	0.4465	0.6285
UPE-Rnf-20% of CIFs-*g*-poly(AAc)	4.13	9.51	13.26	20.99	29.56	36.29	0.0089	0.1115	0.2863	0.3412	0.4781	0.6759

Table 7: % Moisture absorption shown by neat UPE, UPE-Rnf-raw CIFs, and UPE-Rnf-CIFs-*g*-poly(AAc) at different humidity levels

Sample designation	% Humidity levels		
	20	50	80
Virgin UPE	0.08	0.11	0.25
UPE-Rnf-20% of raw CIFs	0.46	0.67	0.86
UPE-Rnf-20% of CIFs-*g*-poly(AAc)	0.45	0.65	0.84

Pure polyester resin exhibited low % of water and moisture absorption than raw CIFs and CIFs-*g*-poly(AAc)-fortified polyester composites because of the non-hydrophilic nature of the polymer matrix. However, the introduction of raw CIFs and CIFs-*g*-poly(AAc) copolymers in polymer matrix causes enhancement in moisture absorption and % water absorption behavior. This might be because of the formation of hydrogen bonding and increased Van der walls interaction between water molecules and hydrophilic biofiber, which have been exposed at the surface of composite samples to the outer environment. Further, negligible improvement was observed on moisture absorption and water absorption after surface functionalization of CIFs.

The chemical resistance of pure polymer matrix and composite specimens toward acid and alkali decreases with an increase in normality as well as with the time of contact and has been observed better against acids in contrast to the base. If we compare the stability of different polymer composite specimens against chemicals, then we observe that the neat polyester matrix is highly stable followed by CIFs-fortified and CIFs-*g*-poly(AAc)-fortified polyester composites. The poor stability of CIFs-*g*-poly(AAc)-fortified polyester composites could be because of the dissolution of grafted AAc chains in acidic/basic medium (49), which will lead to the deep penetration of acid/base in the specimen, and thus ultimate failure of specimens has been noticed. In addition, poor chemical resistance of raw CIFs-fortified polyester composite than virgin matrix was also noticed, which may be due to the removal of waxes and hemicelluloses contents from fibers' surface and deep penetration of chemicals.

7 Biodegradability study

The percent biodegradability or biodegradation of the pure matrix, and raw and CIFs-*g*-poly(AAc)-fortified composite specimens have been depicted in Figure 6. From the figure, it has been found that biodegradation of the polyester matrix enhances fortification with raw and surface-tailored CIFs. However, between raw CIFs and CIFs-*g*-poly(AAc) co-polymers, the former one was noticed to have better biodegradation.

The inferior biodegradation of CIFs-*g*-poly(AAc)-fortified UPE bio-composites could be because of the improved interaction between surface tailored fibers and matrix, which will lessen exposure of CIFs to the outer atmosphere and hence will result in a decrement in the biodegradation. In addition, decrement in biodegradation of surface tailored

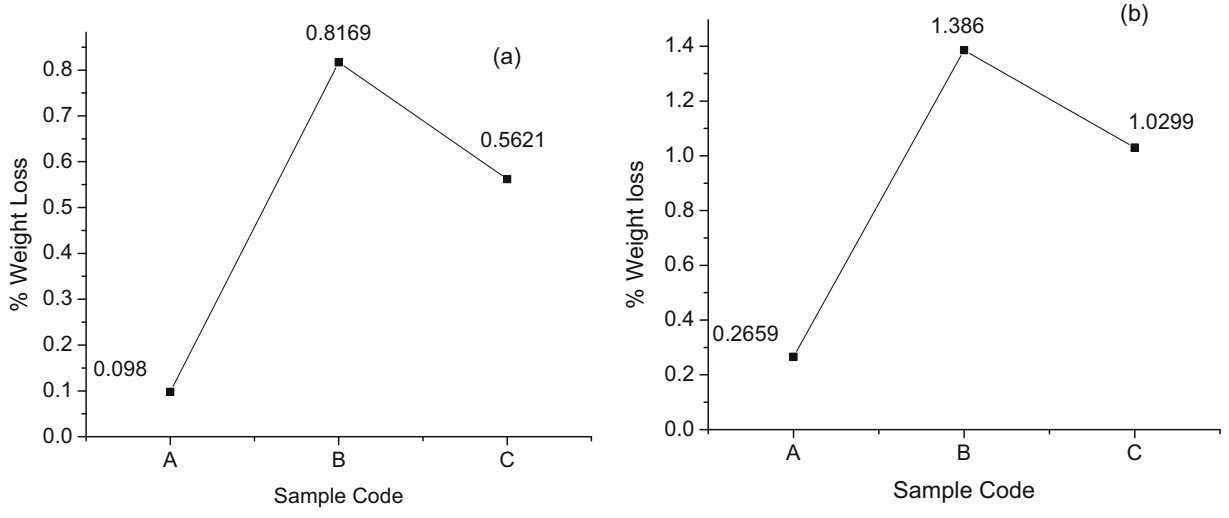

Figure 6: % Weight loss of composite specimens after (a) 6 and (b) 12 months (A, B, and C stands for pure matrix, raw CIFs-fortified UPE composites, and CIFs-*g*-poly(AAc) strengthen UPE composite samples, respectively).

fibers fortified polyester may be assigned due to non-biodegradable nature of grafted vinyl chains onto biofibers.

8 Conclusion

From the above investigations, it has been noticed that compressive, tensile, and flexural strengths of UPE matrix improve after fortification (20 wt%) with the raw CIFs, and were found to further enhance by 11.02%, 10.61%, and 11.04%, respectively, after surface tailoring of fibers. Further, the dielectric constant, dielectric strength, and physicochemical properties of UPE resin, have been found to decline after fortification of UPE matrix with biofibers; however, between raw CIFs and CIFs-*g*-poly(AAc) reinforced composite, better results were found with CIFs-*g*-poly(AAc) graft copolymers. Also, during the evaluation of moisture and water absorption characteristics of raw and functionalized CIFs-based polymer composites, it has been noticed that the latter is comparatively better resistant to moisture/water molecules. However, low chemical stability for CIFs-*g*-poly(AAc) graft copolymers-fortified UPE composites was observed against acid and base as compared to neat and raw CIFs strengthen UPE matrix. The fire resistance characteristics of the matrix were found to be increased after fortification with raw fibers and have been noticed to further enhance after fortification with surface functionalized fibers. However, a negligible impact was observed on fire retardancy after the addition of fire retardants. Further, an increase in biodegradation of matrix has also been noticed with the addition of bio-fillers.

The motive of the present work was to explore the reinforcing ability of underutilized CIFs and to evaluate the impact of graft copolymerization technique on the properties of the resulted UPE matrix-based composites. Since during the study, we have noticed that CIFs has the tremendous reinforcing ability and also leads to enhancement in thermal, dielectric, and fire-resistant properties of polyester composites, these UPE resin-based polymer composites play a remarkable role in polymer composite industries more particularly in fabricating of automobile parts, dielectric materials, building materials, and door panels.

Acknowledgements: The authors wish to thank their parental institutes for providing the laboratory facilities to accomplish this work. Vijay Kumar Thakur would like to thank the research support provided by the Royal Academy of Engineering (IAPP18-19\295) and UKIERI (DST/INT/UK/P-164/2017).

Funding information: Research support provided by the Royal Academy of Engineering (IAPP18-19\295) and UKIERI (DST/INT/UK/P-164/2017).

Author contributions: Ashvinder Kumar: writing – original draft, methodology, and formal analysis; Vijay Kumar Thakur: writing – original draft, formal analysis, visualization, and project administration; Amar Singh Singha: resources and supervisions.

Conflict of interest: Authors state no conflict of interest.

References

(1) Li M, Pu Y, Thomas VM, Yoo CG, Ozcan S, Deng Y, et al. Recent advancements of plant-based natural fiber-reinforced composites and their applications. Compos Part B Eng. 2020;200:108254. doi: 10.1016/j.compositesb.2020.108254.
(2) Gopinath V, Saravanan S, Al-Maleki AR, Ramesh M, Vadivelu J. A review of natural polysaccharides for drug delivery applications: special focus on cellulose, starch and glycogen. Biomed Pharmacother. 2018;107:96–108.
(3) Daminabo SC, Goel S, Grammatikos SA, Nezhad HY, Thakur VK. Fused deposition modeling-based additive manufacturing (3D printing): techniques for polymer material systems. Mater Today Chem. 2020;16:100248. doi: 10.1016/j.mtchem.2020.100248.
(4) Joshi S, Rawat K, Karunakaran C, Rajamohan V, Mathew AT, Koziol K, et al. 4D printing of materials for the future: Opportunities and challenges. Appl Mater Today. 2020;18:100490. doi: 10.1016/j.apmt.2019.100490.
(5) Dubey SP, Thakur VK, Krishnaswamy S, Abhyankar HA, Marchante V, Brighton JL. Progress in environmental-friendly polymer nanocomposite material from PLA: synthesis, processing and applications. Vacuum. 2017;146:655–63. doi: 10.1016/j.vacuum.2017.07.009.
(6) Pickering KL, Efendy MA, Le TM. A review of recent developments in natural fibre composites and their mechanical performance. Compos Part A Appl Sci Manuf. 2016;83:98–112.
(7) Ramesh M, Palanikumar K, Reddy KH. Plant fibre based bio-composites: sustainable and renewable green materials. Renew Sustain Energy Rev. 2017;79:558–84.
(8) Platnieks O, Sereda A, Gaidukovs S, Thakur VK, Barkane A, Gaidukova G, et al. Adding value to poly (butylene succinate) and nanofibrillated cellulose-based sustainable nanocomposites by applying masterbatch process. Ind Crop Products. 2021;169:113669. doi: 10.1016/j.indcrop.2021.113669.
(9) Singha AS, Thakur VK. Synthesis, characterisation and analysis of Hibiscus Sabdariffa fibre reinforced polymer matrix-based composites. Polym Polym Compos. 2009;17(3):189–94. doi: 10.1177/096739110901700308.
(10) Singha AS, Thakur VK. Fabrication of Hibiscus sabdariffa fibre reinforced polymer composites. Iran Polym J. 2008;17(7):541–53.

(11) Berni R, Cai G, Hausman J-F, Guerriero G. Plant fibers and phenolics: a review on their synthesis, analysis and combined use for biomaterials with new properties. Fibers. 2019;7(9):80.
(12) Ramesh M, Deepa C, Kumar LR, Sanjay MR, Siengchin S. Life-cycle and environmental impact assessments on processing of plant fibres and its bio-composites: a critical review. J Ind Text. 2020;1528083720924730.
(13) Singha AS, Thakur VK. Grewia optiva fiber reinforced novel, low cost polymer composites. E-J Chem. 2009;6(1):71–6. doi: 10.1155/2009/642946.
(14) Siwal SS, Zhang Q, Devi N, Saini AK, Saini V, Pareek B, et al. Recovery processes of sustainable energy using different biomass and wastes. Renew Sustain Energy Rev. 2021;150:111483. doi: 10.1016/j.rser.2021.111483.
(15) Rana A, Thakur VK. Bright side of cellulosic Hibiscus Sabdariffa fibres: towards sustainable materials from macro to nanoscale. Mater Adv. 2021;2(15):4945–65.
(16) Rana AK, Potluri P, Thakur VK. Cellulosic Grewia optiva fibres: towards chemistry, surface engineering and sustainable materials. J Environ Chem Eng. 2021;9(5):106059.
(17) Beluns S, Gaidukovs S, Platnieks O, Gaidukova G, Mierina I, Grase L, et al. From Wood and Hemp Biomass Wastes to Sustainable Nanocellulose Foams. Ind Crop Products. 2021;170:113780.
(18) Singha AS, Thakur VK. Physical, chemical and mechanical properties of Hibiscus sabdariffa fiber/polymer composite. Int J Polym Mater Poly Biomater. 2009;58(4):217–28. doi: 10.1080/00914030802639999.
(19) Namvar F, Jawaid M, Tanir PM, Mohamad R, Azizi S, Khodavandi A, et al. Potential use of plant fibres and their composites for biomedical applications. BioResources. 2014;9(3):5688–706.
(20) Thakur VK, Singha AS, Thakur MK. In-air graft copolymerization of ethyl acrylate onto natural cellulosic polymers. Int J Polym Anal Charact. 2012;17(1):48–60. doi: 10.1080/1023666X.2012.638470.
(21) Thakur VK, Singha AS, Thakur MK. Fabrication and physico-chemical properties of high-performance pine needles/green polymer composites. Int J Polym Mater Polym Biomater. 2013;62(4):226–30. doi: 10.1080/00914037.2011.641694.
(22) Rana AK, Frollini E, Thakur VK. Cellulose nanocrystals: Pretreatments, preparation strategies, and surface functionalization. Int J Biol Macromol. 2021;182:1554–81.
(23) Thakur VK, Singha AS, Misra BN. Graft copolymerization of methyl methacrylate onto cellulosic biofibers. J Appl Polym Sci. 2011;122(1):532–44. doi: 10.1002/app.34094.
(24) Singha AS, Rana AK. Improvement of interfacial adhesion in Cannabis indica/unsaturated polyester biocomposites through esterification reaction. Int J Polym Anal Charact. 2012;17(8):590–9.
(25) Singha AS, Rana AK. Preparation and characterization of graft copolymerized Cannabis indica L. fiber-reinforced unsaturated polyester matrix-based biocomposites. J Reinforced Plast Compos. 2012;31(22):1538–53.
(26) Rana AK, Singha AS. Dielectric, flammability and physico-chemical properties of surface functionalized Cannabis indica fibers reinforced composite materials. Polym Sci Ser A. 2015;57(2):221–32. doi: 10.1134/S0965545X15020145.
(27) Manaia JP, Manaia AT, Rodriges L. Industrial hemp fibers: an overview. Fibers. 2019;7(12):106. doi: 10.3390/fib7120106.
(28) Lee CH, Khalina A, Lee SH, Liu M. A comprehensive review on bast fibre retting process for optimal performance in fibre-reinforced polymer composites. Adv Mater Sci Eng. 2020;2020:e6074063. doi: 10.1155/2020/6074063.
(29) Pappu A, Pickering KL, Thakur VK. Manufacturing and characterization of sustainable hybrid composites using sisal and hemp fibres as reinforcement of poly (lactic acid) via injection moulding. Ind Crop Products. 2019;137:260–9. doi: 10.1016/j.indcrop.2019.05.040.
(30) Väisänen T, Heikkinen J, Tomppo L, Lappalainen R. Improving the properties of wood–plastic composite through addition of hardwood pyrolysis liquid. J Thermoplast Composite Mater. 2016;29(11):1587–98.
(31) Dhakal HN, Zhang Z. The use of hemp fibres as reinforcements in composites. Biofiber Reinf Composite Mater. 2015;86–103.
(32) Singha AS, Thakur VK. Synthesis and characterization of pine needles-reinforced RF matrix-based biocomposites. E-J Chem. 2008;5(S1):1055–62. doi: 10.1155/2008/395827 (Accessed: 30th December 2020).
(33) Singha AS, Shama A, Thakur VK. X-Ray diffraction, morphological, and thermal studies on methylmethacrylate graft copolymerized Saccharum ciliare fiber. Int J Polym Anal Charact. 2008;13(6):447–62. doi: 10.1080/10236660802399747.
(34) Cruz J, Fangueiro R. Surface modification of natural fibers: a review. Proc Eng. 2016;155:285–8. doi: 10.1016/j.proeng.2016.08.030.
(35) Banea MD, Neto JSS, Cavalcanti DKK. Recent trends in surface modification of natural fibres for their use in green composites. In: Thomas S, Balakrishnan P, editors. Green Composites. Singapore: Springer; 2021. p. 329–50. doi: 10.1007/978-981-15-9643-8_12 (Accessed: 25th April 2021).
(36) Mukhopadhyay S, Fangueiro R. Physical modification of natural fibers and thermoplastic films for composites – a review. J Thermoplast Composite Mater. 2009;22(2):135–62. doi: 10.1177/0892705708091860.
(37) Atmakuri A, Palevicius A, Vilkauskas A, Janusas G. Review of hybrid fiber-based composites with nano particles – material properties and applications. Polymers. 2020;12(9):2088.
(38) Gao Y, Romero P, Zhang H, Huang M, Lai F. Unsaturated polyester resin concrete: a review. Constr Build Mater. 2019;228:116709. doi: 10.1016/j.conbuildmat.2019.116709.
(39) Conzatti L, Giunco F, Stagnaro P, Capobianco M, Castellano M, Marsano E. Polyester-based biocomposites containing wool fibres. Compos Part A Appl Sci Manuf. 2012;43(7):1113–9. doi: 10.1016/j.compositesa.2012.02.019.
(40) Prasad AR, Rao KM. Mechanical properties of natural fibre-reinforced polyester composites: Jowar, sisal and bamboo. Mater Des. 2011;32(8–9):4658–63.
(41) Chabros A, Gawdzik B, Podkościelna B, Goliszek M, Pączkowski P. Composites of unsaturated polyester resins with microcrystalline cellulose and its derivatives. Materials. 2020;13(1):62.
(42) Singha AS, Rana AK, Jarial RK. Mechanical, dielectric and thermal properties of Grewia optiva fibers-reinforced unsaturated polyester matrix-based composites. Mater & Des. 2013;51:924–34. doi: 10.1016/j.matdes.2013.04.035.
(43) Singha AS, Rana AK. Kinetics of graft copolymerization of acrylic acid onto cannabis indica fibre. Iran Polym J. 2011;20:913–29.

(44) Severini F, Gallo R. Differential scanning calorimetry study of the thermal decomposition of peroxides in the absence of a solvent. J Therm Anal. 1985;30(4):841–7.
(45) Bledzki AK, Lucka M, Al Mamun A, Michalski J. Biological and electrical resistance of acetylated flax fibre-reinforced polypropylene composites. Bioresources. 2009;4(1):111–25.
(46) Pothan LA, Simon F, Spange S, Thomas S. XPS studies of chemically modified banana fibers. Biomacromolecules. 2006;7(3):892–8.
(47) Chand N, Jain D. Effect of sisal fibre orientation on electrical properties of sisal fibre-reinforced epoxy composites. Compos Part A Appl Sci Manuf. 2005;36(5):594–602.
(48) Kipcak AS, Baran Acarali N, Moroydor Derun E, Tugrul N, Piskin S. Effect of magnesium borates on the fire-retarding properties of zinc borates. J Chem. 2014;2014:512164.
(49) Giri G, Nanda CN, Samal RK. Graft copolymerization onto wool fibers: graft copolymerization of acrylic acid onto wool fibers initiated by quinquivalent vanadium. Polym J. 1989;21(11):883–93. doi: 10.1295/polymj.21.883.